Cyclic Voltammetry Studies of PEO Processes in Alkaline and Silicate/Phosphate Electrolytes and Resulting Coatings

Husein Meshreghi[1*], M. Gorbatkov[2], A. Yerokhin[3], A. Matthews[3]
[1] haaal112@hotmail.com, [2] mikesg@mail.ru, [3] aleksey.yerokhin@manchester.ac.uk, [3]allan.matthews@manchester.ac.uk
[1] Chemical Engineering, Sok Alkhamis Imsehel High Tec. Institute, Tripoli, Libya
[2] Ufa State Aviation Technical University, 12 Karl Marx Street, Russian Federation
[3] Department of Materials, University of Manchester, M139PL, United Kingdom
*HAAAL112@hotmail.com

ABSTRACT

A cyclic voltammetry (CV) method was employed to clarify the electrochemical behaviour of Al in alkaline silicate/phosphate electrolytes over a voltage range of 0 to 550V and study the growth process of plasma electrolytic oxidation (PEO) coatings on rectangular shape Al foil samples. The non-linear behaviour of the current – voltage curve reflects a combination of three processes, including dissolution, passivation and formation of PEO coating under discharge conditions. Different thickness distributions of oxide layer and residual aluminium along the sample length were observed. Similarly, the total Al consumed for the coating process at the edge of sample was more than in the middle. Silicate addition obstruct anodic dissolution of Al, which enhanced the oxide growth. While phosphate, in addition of promoting alpha phase formation it is also enhancing strong metal passivation and allow the breakdown voltage to be easily obtained. Breakdown voltage depends on the concentration and electrolyte composition. Under the studied conditions, we can also conclude that the sparking voltage decreases when electrolyte resistivity decrease which is consistent with Ikonopisov equation. However, which's more surprising and unexpected in K electrolyte, is the earlier emission starting prior to the current starts increasing. There are a number of considerations used to determine the breakdown voltage such as reaching of maximum voltage, rapid voltage fluctuation. However, the appearance of visible sparking is not a criteria for detecting the dielectric breakdown as concluded in our study although many literatures considered this as criteria.

Keywords: Cyclic, Concentration, electrochemical, linear, plasma, thickness

1. Introduction

Plasma electrolytic oxidation is electrochemical conversion of a metal surface to produce an oxide ceramic layer [1, 2]. The PEO process is a complex process including concurrent partial processes of oxide layer formation, dissolution and dielectric breakdown. For example, several researchers used a number of considerations to define the breakdown voltage. They found, in addition of type of working electrode the sparking voltage depends on concentration, composition and temperature of electrolyte and current density. The CV method was used to understand and identify the potential variations corresponding to differential behaviour of Al foil electrodes during the process which is very helpful in clarifying the mechanisms of the coatings formation [3]. Although, there are several factors

that affect coating thickness uniformity, such as current mode and density, electrolyte pH, composition and concentration as well as chemical composition of the substrate, the electrolyte plays a very important role in the PEO process. Electrolytes used usually promote metal passivation by forming a thin insulating surface layer which provides a prerequisite for the dielectric breakdown to induce spark discharge [4-7]. Some additives such as silicates, phosphates and aluminates are widely used as basic ingredients of the electrolytes to enhance metal passivation and facilitate sparking. These additives may increase either electrolyte conductivity, thus reducing the breakdown voltage, or the quality of the ceramic coating. This is reflected in current and voltage transients which have been widely studied to reveal the electrode surface state and underpinning electrochemical processes, such as anodic dissolution and film growth [4, 8]. For instance, an increase in alkaline electrolyte solution concentration of KOH from 0.5 to 2 g/L was found to lead to decreases the film growth rate and increases in the rate of anodic dissolution due to the chemical attack by hydroxide ions OH^-. Often in the literature, the PEO process has been subdivided into two to four different stages [9-11]. However, the explanations are not always consistent and not all of these stages are always clearly identifiable in the electrical transients. In the presence of oxide film on aluminium surface, the anodic dissolution of aluminium may be categorised into two types. The first one is a direct metal dissolution reaction by movement of aluminium ions through the oxide layer, while the second is an indirect metal dissolution reaction by consecutive electrochemical film formation at the metal/oxide interface, owing to the movement of OH^- through the film towards aluminium, and chemical film dissolution due to OH^- attack at the film/solution interface [12]. It is also often assumed that OH^- could also get deprotonated at the oxide-electrolyte interface and O^{2-} ions would then provide a much greater fraction of the anionic flow. Discussing the mechanism of anodic dissolution of aluminium in alkaline media, Moon and Prabhu stated that the direct metal dissolution, which involves direct ejection of aluminium ions from the film into the solution definitely does not occur in alkaline solutions, due to the instability of aluminium ions because aluminium ions are not stable thermodynamically in alkaline solution [12]. Therefore, for analyse the dissolution mechanism of pure aluminium in alkaline solution, it will be sufficient to consider indirect working electrode dissolution by consecutive oxide layer formation.

Thickness variations of PEO coating on Al are often observed. Although the chemical composition and microstructure including (crystal structure, crystalline size, orientation, defects and density) are the factors affecting mechanical properties of the coatings, these are also strongly influenced by the coating thickness. Several authors discussing the importance of the coating thickness in the mechanical properties of PEO coatings stated that thicker coatings usually show better mechanical properties[13, 14], however this is not always true as the defects such as porosity may play crucial rule in the mechanical performance of thick PEO coatings. Design engineers specify thickness for various reasons, including some applications which need specific aim, such as the need of a degree of flexibility which influence by the residual metal in the component [15]. The objective of this study is to provide better understanding of the electrochemical behaviour of Al in an alkaline electrolyte with and without silicate and pyrophosphate additives under the

potentials corresponding to those applied in PEO treatments, using cyclic voltammetry (CV) technique. This is also used to understand the coating formation process during the PEO treatment such as the underlying metal-electrolyte interactions.

2. Experiments

Rectangular shape samples of 50 μm thick aluminium foil with dimensions 30 mm × 18 mm × 0.05 mm and surface roughness of *Ra* ~ 0.1 to 0.2 μm were used as substrates. Prior to the treatment, the samples were cleaned in distilled water and acetone and dried by air. The cleaned samples were suspended in the electrolyte using an insulated metal holder. The process was carried out in two different electrolytes (1.25 g/l KOH) and (1.25 g/L KOH, 2.0 g/L $Na_4P_2O_7$, 2.0 g/L Na_2SiO_3) with conductivities of 0.55 and 0.70 S/m and pH values of 11.88 and 12.10 respectively, denoted as K and KSi2P2 electrolytes. The voltage was ramped with a scan rate of 2.44 V sec^{-1} over the range of 0-550 V, corresponding to the conditions of PEO treatment. Figure 1 shows the geometry of the electrolytic cell used in the experiment. It consists of a working electrode sample connected to the positive output a 30 kW DC power supply and a 2-L cylindrical stainless-steel tank with inside diameter of 130 mm and height of 145 mm, which served as a cathode with surface area of 8.57×10^{-2} m^2, equipped with a stirring and cooling system. The electrolyte temperature was kept within the range of 30 to 35 ^oC. In order to correlate optical emission and physicochemical processes on the sample surface during the PEO treatment, optical emission spectroscopy (OES) study was carried out using a FloTron XHR spectrometer operated in the range from 300 to 900 nm wavelength range with a resolution of 1.8 nm. To evaluate the distribution and thickness of the PEO coating on the Al foil, SEM images were taken along the length of the whole sample.

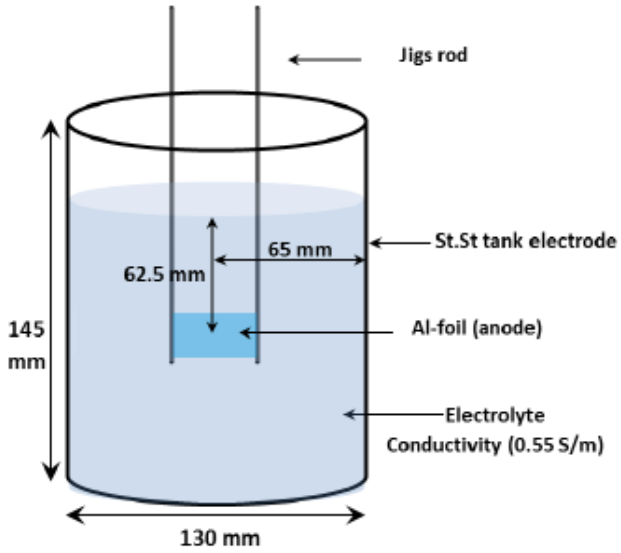

Figure 1. *The electrolytic cell used in the studies of the PEO process.*

The Images were obtained at 2000x and 5000x magnification using an Inspect F50 SEM operated at a 15 kV accelerating voltage and 10.8 mm working distance. The size of the images was 1024×943 pixel. A MountainsMap 7.1 and ImagJ software were used to analyse the SEM images.

3. Results and Discussion

3.1. Formation Mechanism of PEO Coatings

Figure 2 shows the current density-voltage responses obtained from CV experiments corresponding to the conditions of PEO treatment in the K and KSi2P2 electrolyte.

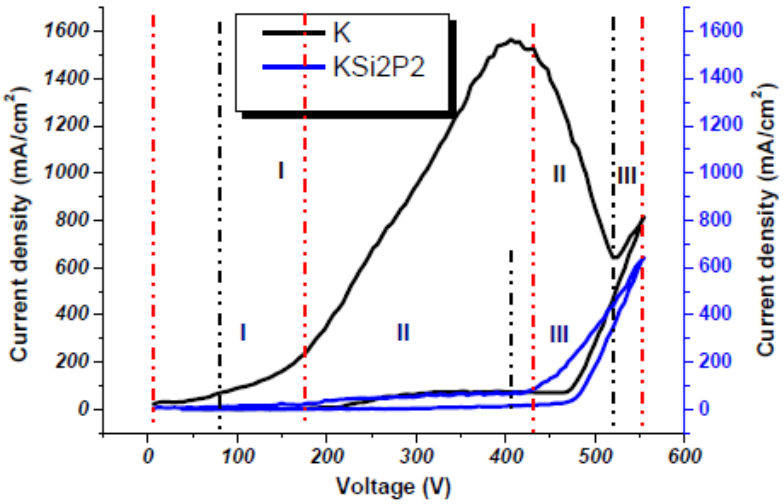

Figure 2. *Current density-voltage characteristics of PEO process of aluminium foil in K and KSi2P2 electrolytes*

Often in the literature, the PEO process has been subdivided into two to four different stages[1, 9, 10]. However, the explanation of the different stages is not always the same and not always clearly identifiable in the voltage-time response diagrams. The anodic reaction on the surface of aluminium foil sample treated in K electrolyte is considered as indirect metal dissolution and the hydroxide film formation starts electrochemically on the surface of aluminium by migration of hydroxide ions through the aluminium/film interface. The following reactions are suggested to explain the mechanism of dissolution and formation of the PEO coating:

$$Al + 3OH^- \rightarrow Al(OH)_3 + 3e^- \quad (1)$$

The aluminium hydroxide film which formed electrochemically will be dissolved chemically by an attack of OH^- ions at the film/solution interface and form aluminate ions $Al(OH)4^-$ as:

$$Al(OH)_3 + OH \rightarrow Al(OH)_4^- \quad (2)$$

Additionally, as a result of aluminium anodic dissolution, hydrogen evolution takes place as (Eq 3):

$$Al + 3H_2O + OH \rightarrow \frac{3}{2}H_2O + AlOH_4^- \quad (3)$$

The curve K in Figure 2 appears to be composed of three stages. The first stage I (0-380V) corresponds the steep climb of current density to the peak of about 1550 mA/cm². Certainly, that the increase of the current density in the first stage is due to the anodic dissolution occurred on the surface of aluminium (Eqs. 1&2). Pyun and Moon [10] stated

in that the increasing rotation rate of the sample causes fast supply of OH^- ions to the film/solution interface and rapid removal of aluminate ions $Al(OH)^{4-}$ away from the film solution interface. At the oxide/electrolyte interface, the oxygen evolution is quite common for aluminium anodising in alkaline solution. Also, the potential is very high and the water splitting potential is already passed. Therefore, it may either have other reactions due to the water splitting which is caused by high voltage where the OH^- anions are absorbed on the surface, (Eq. 1) and direct combination of Al and O atoms in plasma state under the effect of spark discharge, (Eqs. 4-5) [16, 17]

$$4OH^- \rightarrow O_2^- \uparrow + 2H_2O + 4e^- \quad (4)$$

$$2Al_{ejected} + 6OH^- \rightarrow Al_2O_3 + 3H_2O + 6e^- \quad (5)$$

The stage II Figure 2 shows a more complex behaviour, where reaction rates may be affected by mass transport, in particular, how fast the species can depart from the surface of the sample. That means, if the species depart slowly this will hold the reactions and dissolution is offset by transport limitations, not by the barrier-type anodic film formed. So, the current eventually becomes reduced as seen in Figure 2, and even independent of potential. When the electric field strength was strong enough, the breakdown voltage and dielectric breakdown take place across the oxide film at around ~535V, accompanied with numerous of spark discharges. Hereafter, the current density climbed steadily as seen in stage III (535-560V). During this stage, the main reactions that occur on the aluminium electrode are associated with transformation of the hydrated anodic oxide to ceramic alumina and combination of aluminium and oxygen atoms in plasma state under the influence of spark discharge, also to form alumina [1, 4].

According to Figure 2, addition of 2 g/l for both Na_2SiO_3 and $Na_4P_2O_7$ to 1.25g/l KOH electrolyte shows completely different current-voltage behaviour. Adding silicates and pyrophosphates to alkaline electrolytes is commonly used to promote metal surface passivation due to the formation of insoluble compounds and allow the sparking voltage to be easily reached which is the most beneficial for the coating production by the PEO process. The cyclic voltammetry curve for KSi2P2 electrolyte in Figure 2 does not actually shows evidence of anodic dissolution, although it also displays three distinguished stages according to the applied voltage. Stage I (0-150V), indicating no significant current density change due to the fact that the formation rate of the passive oxide layer takes control over the metal dissolution rate on the surface. The second stage II (150-425V) corresponds the slight increase in current density with applied voltage to peak at about 100 mA/cm^2. At around ~425V, the current increases and the electric field strength in the oxide film reaches a critical value which causes dielectric breakdown of the oxide film. In the stage III (425-550V), the current density increases sharply with increasing voltage. As shown in Figure 2, addition of sodium silicate leads to production of SiO_2 due to the transport of SiO_3^{2-} anions towards the coating/electrolyte interface during the PEO process. The silica produced may inhibit the release of Al^{3+} cations, leading to a decrease in breakdown voltage. In other side, the electrolyte may include substances which enhance to decrease the electrolyte resistivity such as sodium hydroxide or potassium hydroxide (1-50 g/l) [4].

This according to Ikonopisov equation [18] could be cause the decreasing of breakdown voltage. The following reactions (Eqs. 6-7) are suggested for the formation of such silica.

$$SiO_3^{2-} + 2H^+ \rightarrow SiO_2 + H_2O \quad (6)$$

$$SiO_3^{2-} + 2H^+ + (n-1)H_2O \rightarrow SiO_2nH_2O \quad (7)$$

3.2. Relationships Between OES and Current-Voltage Behaviour

Figure 3 displays the recorded spectrum of optical emission from the exposed area of the plasma discharge during the PEO process in K and KSi2P2 electrolytes which contain aluminium (Al 309 and Al 396 nm) from substrate and potassium, sodium, and hydrogen α and β (K-765, Na-589, H_α-656 nm and H_β) lines from electrolytes. In this experiment, OES signal with the wavelength shorter than 300 nm cannot be registered, because it is absorbed by the electrolyte. As seen in Figure 3, for samples treated in both electrolytes, the strongest observed lines correspond to aluminum (Al-396 nm) and (H_α-656 nm). While the relatively low intensities were recorded from potassium (K-765 nm) and (H_β- 486 nm). In addition, sodium line (Na-589 nm) arises in the spectra of microdischarges on the sample treated in the KSi2P2 electrolyte.

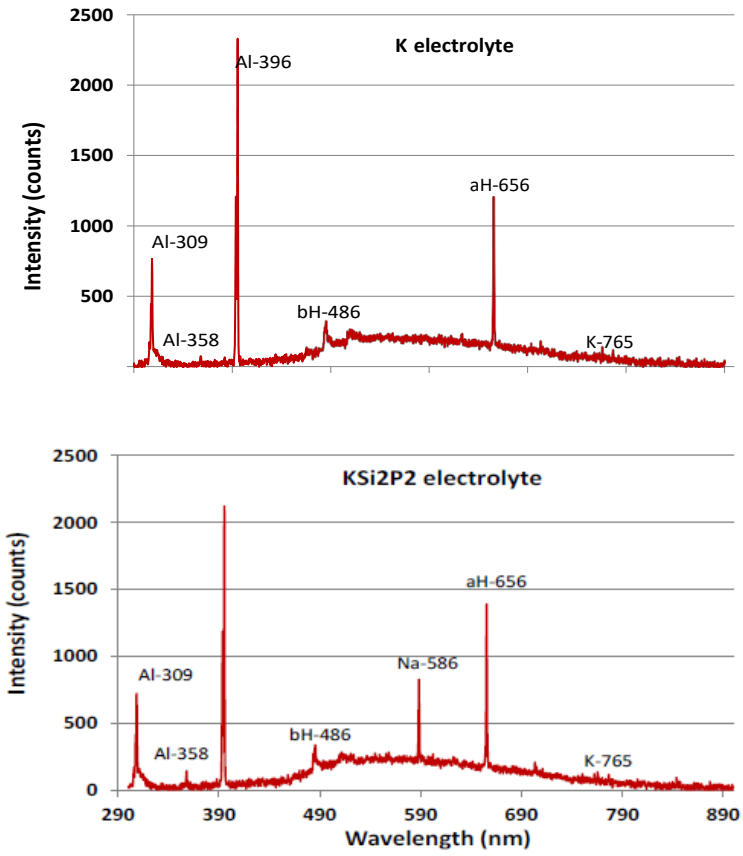

Figure 3. *Optical emission spectrum during the PEO process on Al foil in K and KSi2P2 electrolytes.*

Evolution of emission line intensities with the treatment time in CV mode is presented in Figure 4. Differences OES signal during treatments in K and KSi2P2 electrolytes are

attributed to the additions of silicate and phosphate to the electrolyte. The OES signals of samples treated in K electrolyte become visible after about 205 sec to reach voltage 525 V for 0.8 A/cm² and ended after around 255 sec to reach voltage around 460 V for 0.1 A/cm². While signals of samples treated in KSi2P2 electrolyte started after 175 sec with voltage 425 V for 0.1 A/cm² and ended at the same time as for the sample treated in K electrolyte with voltage 480 V for 0.01 A/cm². The time to reach the breakdown voltage was significantly shorter in the electrolyte solution containing silicate compared with that without, which is consistent with the analysis of the electrical breakdown phenomenon reported by R.K. Nigam *et al* [19]. Results in Figure 5 shows the atomic line intensity - voltage diagrams plotted in the same scale as the current density - voltage diagrams of Al foil in (a) K and (b) KSi2P2 electrolytes. A comparison of the curves in Figure 6 (a&b) showed dissimilar behaviour of emission intensity lines and a considerable difference in values of current densities at the discharge ignition during the two PEO treatments at the same voltages. Generally, the discharge in PEO process takes place when the applied voltage reaches a specific value corresponding to the breakdown of the oxide layer formed on the sample surface, which causes a generation of intense light emission at the microdischarge sites.

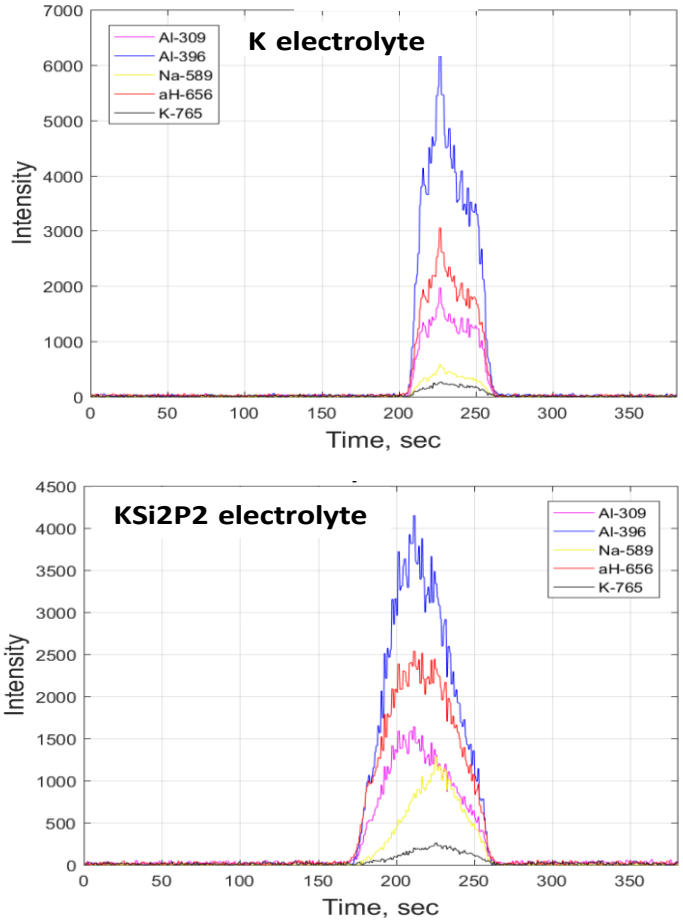

Figure 4. *Typical time variation of the emission line intensity during CV studies of the PEO processes in (a) K and (b) KSi2P2 electrolytes*

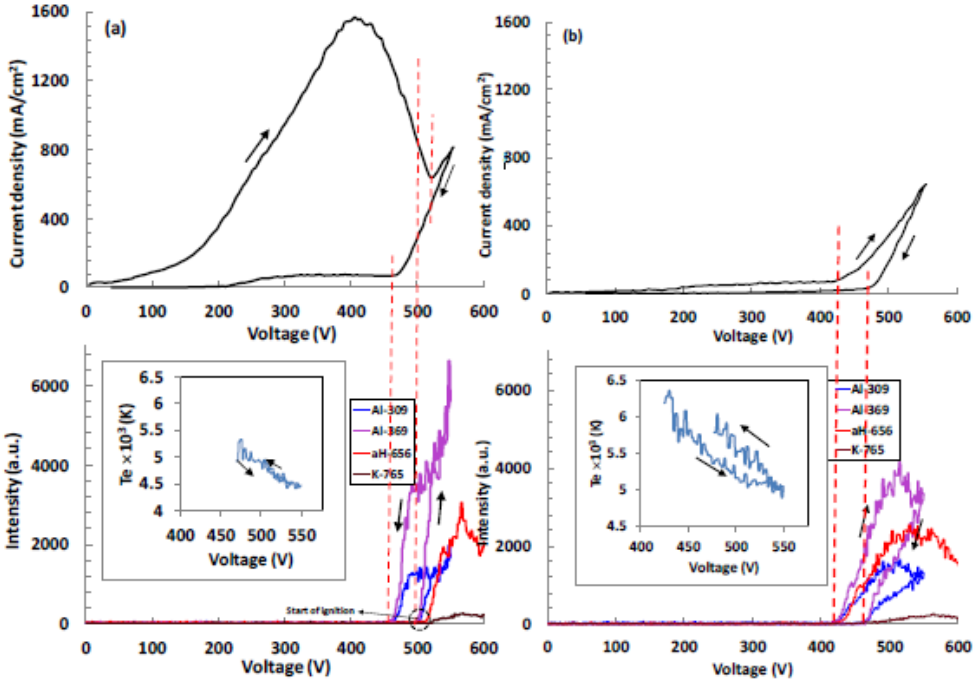

Figure 5. *Plots of intensity versus voltage during the PEO process at same scale with current density versus voltage of Al foil in (a) K and (b) KSi2P2 electrolytes.*

However as seen in Figure 5 (a) the OES signals of the species generated from the sample treated in K electrolyte recorded in the period before the breakdown voltage (535 V) occurs. It is noticed that after the current is fallen and dissolution is offset by transport limitation (not by barrier type), the optical emission observed started prior to the current starts increasing. The ignition and extinction voltages were around 500 V voltage and 460 V respectively, while in K2P2Si2 electrolyte, the OES signal originated at the breakdown voltage (around 425 V) and the extinction voltage is higher (470 V). From Figure 5, it can also be seen that the breakdown voltage of the sample treated in KSi2P2 is shifted about 110V towards lower values in respect to that of the sample treated in K electrolyte, however corresponding values of current densities show opposite trend, 0.8 $A\ cm^{-2}$ versus 0.085 $A\ cm^{-2}$ for the samples treated in K and KSi2P2 electrolyte respectively. In K-electrolyte condition at voltage 425 V there was a fluctuation in the electron plasma temperature (4800 to 5200 K) which is corresponding to the early period of discharges as seen in Figure 5 (a&b). While in K2P2Si2 electrolyte at the same voltage the fluctuation was less at the early stage of sparking (6100-6300). The previous difference could be related to the different in electrolyte conductivity, where the voltage drop at higher electrolyte resistance would means less driving force for the coating to grow, so it means less sparks, less energetic discharge and less plasma temperature. This analysis reflects with what we have from our results in Figure 5 (a&b). It is also displaying the hysteresis of plasma temperature (K) versus voltage (V) in both conditions. Despite a lot of PEO research, how the plasma temperature hysteresis remains not have a good size of analysis and discussion. As can be seen in Figure 5 (a&b) sample treated in K- electrolyte shows a smaller width of Te - V hysteresis than sample treated in KSi2P2 which is not easy to observe. The reason could be related to the substances added to electrolyte K2P2Si2, where the presence of silicate causes substrate passivation by inhibition anodic dissolution

of the Al. So, the above results provided a connection between the electrolyte concentration, plasma temperature and the plasma discharge behaviour.

3.3. Thickness and Uniformity of The Coating Layer

Cross-sectional SEM images of the PEO coatings and residual aluminium layer on the samples treated in K and KSi2P2 electrolytes are shown in Figure 6 ((a)-(b)), respectively. Results show that the PEO coating layer thickness grown in K electrolyte varies from 1.2 ±0.2 µm at edges to 0.6 ±0.2 µm at the middle region of sample. While it ranges from 2±0.2 µm at edges to 1.7±0.2 µm in the middle of the sample treated in KSi2P2 electrolyte. The results show variation in thickness over all surfaces of both samples. However, the coating layer on the sample treated in KSi2P2 electrolyte shows a more uniform coating thickness distribution than that produced in K electrolyte (Figure 7).

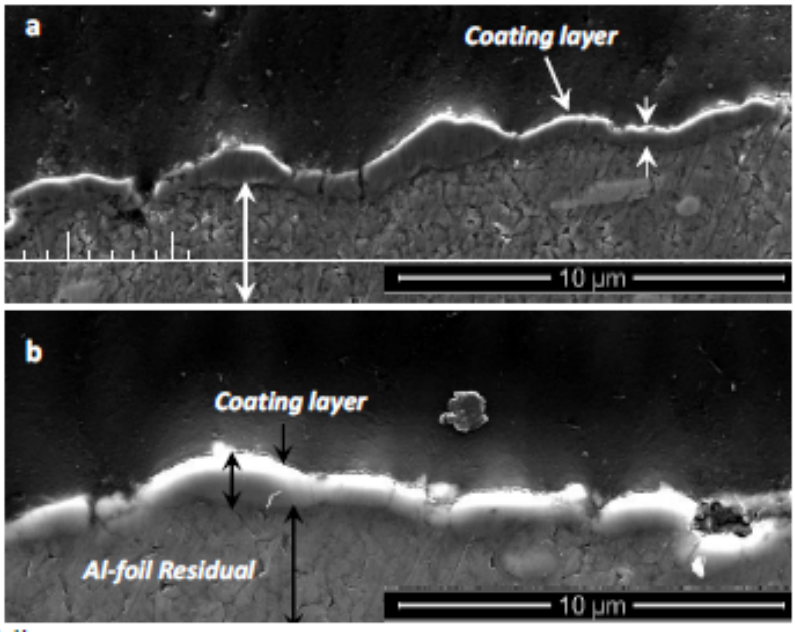

Figure 6. *SEM cross-sectional micrographs of the PEO surface layer on the samples treated in (a) K and (b) KSi2P2 electrolytes*

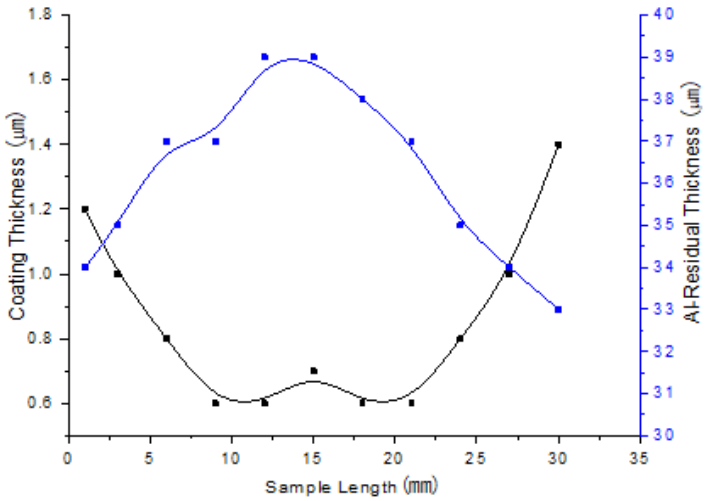

Figure 7. *Thickness distributions of PEO coating and residual Al along the length of the sample treated in K electrolyte.*

Residual thicknesses of coating and aluminium, as well as mass of aluminium consumed for dissolution and ejection, all are presented in Table 1. In spite of previous calculated values seem to agree well with the logic impression one get from the SEM, it has to be considered only as an approximation, due to possible errors, such as the true density of the oxide layer forming phase due to present of porosity that can differ significantly from aluminium or its oxide. As can be seen from Figure 7, the thicknesses of oxide layer showed a sharp fall until reaching around 0.6 μm at 7 mm distance from the edge of the sample and before moving steady between 10 and 15 mm, with almost no thickness increase. Then the thickness grows linearly between around 20 mm to 30 mm distance of the sample length. This fluctuation in oxide film thickness also appeared in the thicknesses of residual aluminium and that lost for dissolution during the process along the whole sample, as shown in Figure 8. In general, the relationship between the PEO coating layer thickness and the charge density passed through the sample surface is direct [1], however, in our results the character of this trend differs for the thickness of oxide film and residual aluminium along the sample length. The non-linear rate distribution of anodic dissolution reaction obtained from such analysis of the sample treated in K-electrolyte (Figure 2) could be of great help in investigation why the variations in residual thicknesses of coating and aluminium occurred. In particular, when the current falls sharply from 1550 to 650 mA/cm² at the breakdown voltage, before it starts gradually increasing and following this trend. Also, it should be noted that the OES signal commenced before the minimum current is achieved (Figure 5). This changing behaviour may influence the distribution of the rates of dissolution and precipitation processes over the sample length, which would affect the thickness distribution of the oxide film. In the other hand, the sample treated in KSi2P2 electrolyte showed less variation in coating thickness than that treated in K electrolyte. The decline in the coating thickness from the sample edge to the middle was around 25% while of sample treated in K electrolyte was 50% (Figure 8 & 9). As stressed previously the cyclic voltammetry curve in this case does not show evidence of anodic dissolution. This indicates surface passivation dominates over dissolution due to the presence of silicate and phosphate. It has been reported that the addition of sodium silicate into KOH solution can promote formation coating layer and increase both the thickness of coating and adhesion strength [20, 21].

Table 1 *Results of thicknesses over the length of sample.*

Sample length point (mm)	**Sample treated in K electrolyte**				**Sample treated in Ksi2P2 electrolyte**			
	Total coating thickness (μm)	Al residual thickness (μm)	Al consumed for whole process (g)	Al consumed for dissolution and ejection (g)	Total coating thickness (μm)	Al residual thickness (μm)	Al consumed for whole process (g)	Al consumed for dissolution and ejection (g)
1	2.4	34.0	8×10^{-4}	6.0×10^{-4}	4.0	41	4×10^{-4}	2.0×10^{-4}
3	2.0	35.0	8×10^{-4}	7.0×10^{-4}	4.0	43	3×10^{-4}	1.5×10^{-4}
6	1.6	37.0	6×10^{-4}	5.4×10^{-4}	3.5	45	3×10^{-4}	1.0×10^{-4}
9	1.4	37.0	6×10^{-4}	5.0×10^{-4}	3.5	47	2×10^{-4}	6.0×10^{-4}
12	1.4	39.0	4×10^{-4}	4.1×10^{-4}	2.0	47	2×10^{-4}	8.0×10^{-4}
15	1.4	37.0	4×10^{-4}	6.0×10^{-4}	2.0	46	2×10^{-4}	5.0×10^{-4}

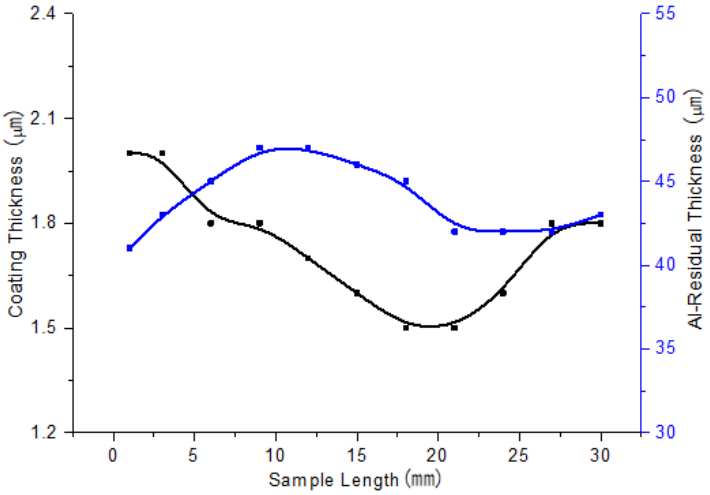

Figure 8. *Distribution of PEO coating and residual Al thicknesses along the length of the sample treated in KSi2P2 electrolyte.*

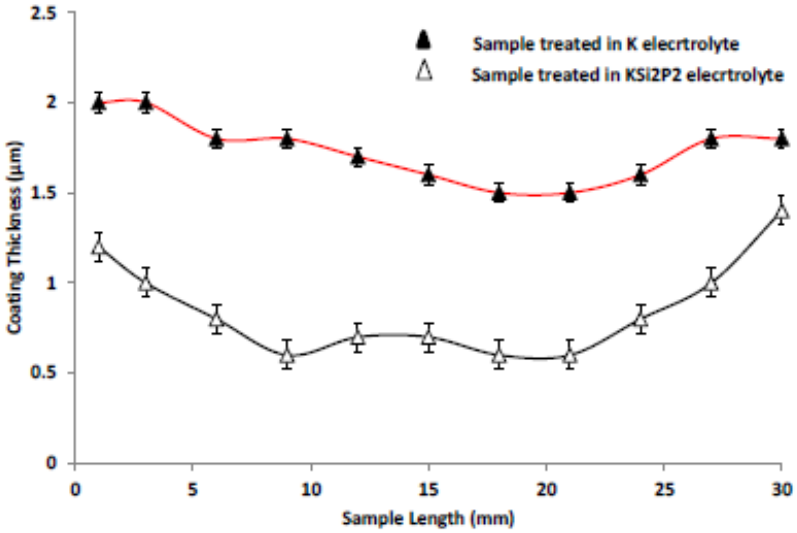

Figure 9. *Oxide layer thickness produced in K and KSi2P2 electrolytes*

4. Conclusions

The non-linear behaviour of the current – voltage curve was observed when using electrolyte without silicate/phosphate. It reflects a combination of three processes, including dissolution, passivation and formation of PEO coating under discharge conditions. Silicate addition obstruct anodic dissolution of Al, which enhanced the oxide growth. While phosphate, in addition of promoting α-Al_2O_3 phase formation it is also enhancing strong metal passivation and allow the breakdown voltage to be easily obtained. Different thickness distributions of oxide layer and residual aluminium along the sample length were observed. Similarly, the total Al consumed for the coating process at the edge of sample was more than in the middle. Under the studied conditions, we can also conclude that the sparking voltage decreases when electrolyte resistivity decrease which is consistent with Ikonopisov equation. However which's more surprising and unexpected in K electrolyte, is the earlier emission starting prior to the current starts increasing.

References

[1] A. Y. L. Snizhko, A. Pilkington, N. Gurevina, D. Misnyankin, A. Leyland , A. Matthews, "Anodic processes in plasma electrolytic oxidation of aluminium in alkaline solutions," *Electrochimica Acta,* vol. 49, no. 13, pp. 2085-2095, 2004.

[2] M. Javidi and H. Fadaee, "Plasma electrolytic oxidation of 2024-T3 aluminum alloy and investigation on microstructure and wear behavior," *Applied Surface Science,* 2013.

[3] A. Ahmadi, P. Norouzi, and M. R. Ganjali, "Study of corrosion resistance of colored anodized aluminum with Quinizarin using cyclic voltammetry and impedance measurement methods," *Progress in Organic Coatings - PROG ORG COATING,* vol. 56, pp. 227-233, 07/01 2006.

[4] A. L. Yerokhin, X. Nie, A. Leyland, A. Matthews, and S. J. Dowey, "Plasma electrolysis for surface engineering," *Surface and Coatings Technology,* 1999.

[5] K. Wang, B.-H. Koo, C.-G. Lee, Y.-J. Kim, S.-H. Lee, and E. Byon, "Effects of electrolytes variation on formation of oxide layers of 6061 Al alloys by plasma electrolytic oxidation," *Transactions of Nonferrous Metals Society of China,* vol. 19, no. 4, pp. 866-870, 2009.

[6] B.-H. Ahn *et al.*, "Effect of Na2SiO3 concentration on the properties of AZ31 magnesium alloy prepared by electrolytic plasma processing," *Electronic Materials Letters,* vol. 9, no. 6, pp. 813-815, 2013.

[7] A. Polat, M. Makaraci, and M. Usta, "Influence of sodium silicate concentration on structural and tribological properties of microarc oxidation coatings on 2017A aluminum alloy substrate," *Journal of Alloys and Compounds,* vol. 504, no. 2, pp. 519-526, 2010.

[8] A. Y. L.Snizhko, A. Pilkington, N. Gurevina, D. Misnyankin, A. Leyland , A. Matthews, "Anodic processes in plasma electrolytic oxidation of aluminium in alkaline solutions," *Electrochimica Acta,* vol. 49, pp. 2085-2095, 2004.

[9] M. Schneider, K. Kremmer, and S. Höhn, "Corrosion protection of thickness reduced plasma electrolytic layers on AZ31," (in English), *MACO Materials and Corrosion,* vol. 67, no. 9, pp. 921-928, 2016.

[10] S.-I. Pyun and S.-M. Moon, "Corrosion mechanism of pure aluminium in aqueous alkaline solution," *Journal of Solid State Electrochemistry,* journal article vol. 4, no. 5, pp. 267-272, 2000.

[11] V. P. Parkhutik, J. M. Martinez-Duart, J. Perrière, A. Climent, Y. E. Makushok, and J. M. Albella, "Electrochemical and plasma anodic oxidation of CdxHg1 − xTe," *Thin Solid Films,* vol. 200, no. 1, pp. 129-138, 5/1/ 1991.

[12] P. Deepa and R. Padmalatha, "Corrosion behaviour of 6063 aluminium alloy in acidic and in alkaline media," *Arabian Journal of Chemistry*.

[13] Z. Han, J. Tian, J. Lao, G. Li, and J. Dai, "Effects of thickness and substrate on the mechanical properties of hard coatings," (in English), *Journal of Coatings Technology and Research,* vol. 1, no. 4, pp. 337-341, 2004.

[14] A. L. H. W. S. X. Nie, A. Yerokhin, S.J. Dowey, A. Matthews, "Thickness effects on the mechanical properties of micro-arc discharge oxide coatings on aluminium alloys," (in English), *Surface and Coatings Technology,* pp. 1055-1060, 1999.

[15] C. Xiaozhou, W. Chao, X. Xiangxin, and C. Gongjin, "Effect of ti addition on the residual aluminium content and mechanical properties of the B4C-al composites produced by vacuum infiltration," (in English), *Arch. Metall. Mater. Archives of Metallurgy and Materials,* vol. 60, 2015.

[16] R. L. Doyle, I. J. Godwin, M. P. Brandon, and M. E. G. Lyons, "Redox and electrochemical water splitting catalytic properties of hydrated metal oxide modified electrodes," *Physical Chemistry Chemical Physics,* 10.1039/C3CP51213D vol. 15, no. 33, pp. 13737-13783, 2013.

[17] H. Duan, Y. Li, Y. Xia, and S. Chen, *Transient Voltage-Current Characteristics: New Insights into Plasma Electrolytic Oxidation Process of Aluminium Alloy*. 2012, pp. 7619-7630.

[18] S. Ikonopisov, *Electrochimica Acta,* vol. 20, no. 783, 1975.

[19] R. K. Nigam, K. C. Singh, and S. Maken, "Electrical breakdown phenomenon and electronic conduction during the anodic growth of Nb 2 O 5," *Can. J. Chem.,* vol. 65, no. 3, pp. 512-517, 1987.

[20] A. Fattah-Alhosseini, M. Vakili-Azghandi, and M. Keshavarz, "Influence of Concentrations of KOH and Na 2 SiO 3 Electrolytes on the Electrochemical Behavior of Ceramic Coatings on 6061 Al Alloy Processed by Plasma Electrolytic Oxidation," *Acta Metall. Sin. (Engl. Lett.),* vol. 29, no. 3, pp. 274-281, 2016.

[21] L. Jung-Hyung and K. Seong-Jong, "Effects of silicate ion concentration on the formation of ceramic oxide layers produced by plasma electrolytic oxidation on Al alloy," (in English), *Japanese Journal of Applied Physics,* vol. 56, no. 1S, 2017.